



CHALMERS

Chalmers Publication Library

Single parity check-coded 16QAM over spatial superchannels in multicore fiber transmission

This document has been downloaded from Chalmers Publication Library (CPL). It is the author's version of a work that was accepted for publication in:

Optics Express (ISSN: 1094-4087)

Citation for the published paper:

Eriksson, T. ; Luis, R. ; Puttnam, B. et al. (2015) "Single parity check-coded 16QAM over spatial superchannels in multicore fiber transmission". Optics Express, vol. 23(11), pp. 14569-14582.

<http://dx.doi.org/10.1364/oe.23.014569>

Downloaded from: <http://publications.lib.chalmers.se/publication/219779>

Notice: Changes introduced as a result of publishing processes such as copy-editing and formatting may not be reflected in this document. For a definitive version of this work, please refer to the published source. Please note that access to the published version might require a subscription.

Chalmers Publication Library (CPL) offers the possibility of retrieving research publications produced at Chalmers University of Technology. It covers all types of publications: articles, dissertations, licentiate theses, masters theses, conference papers, reports etc. Since 2006 it is the official tool for Chalmers official publication statistics. To ensure that Chalmers research results are disseminated as widely as possible, an Open Access Policy has been adopted. The CPL service is administrated and maintained by Chalmers Library.

(article starts on next page)

Single parity check-coded 16QAM over spatial superchannels in multicore fiber transmission

Tobias A. Eriksson,^{1,*} Ruben S. Luís,² Benjamin J. Puttnam,²
José Manuel Delgado Mendinueta,² Peter A. Andrekson,¹
Magnus Karlsson,¹ Yoshinari Awaji,² Naoya Wada,² and Erik Agrell³

¹ Photonics Laboratory, Dept. of Microtechnology and Nanoscience, Chalmers University of Technology, SE-412 96 Gothenburg, Sweden

² Photonic Network Research Institute, National Institute of Information and Communications Technology, Tokyo 184-8795, Japan

³ Dept. of Signals and Systems, Chalmers University of Technology, SE-412 96 Gothenburg, Sweden

*tobias.eriksson@chalmers.se

Abstract: We experimentally investigate single-parity check (SPC) coded spatial superchannels based on polarization-multiplexed 16-ary quadrature amplitude modulation (PM-16QAM) for multicore fiber transmission systems, using a 7-core fiber. We investigate SPC over 1, 2, 4, 5 or 7 cores in a back-to-back configuration and compare the sensitivity to uncoded PM-16QAM, showing that at symbol rates of 20 Gbaud and at a bit-error-rate (BER) of 10^{-3} , the SPC superchannels exhibit sensitivity improvements of 2.7 dB, 2.0 dB, 1.7 dB, 1.3 dB, and 1.1 dB, respectively. We perform both single channel and wavelength division multiplexed (WDM) transmission experiments with 22 GHz channel spacing and 20 Gbaud channel symbol rate for SPC over 1, 3 and 7 cores and compare the results to PM-16QAM with the same spacing and symbol rate. We show that in WDM signals, SPC over h11 core can achieve more than double the transmission distance compared to PM-16QAM at the cost of 0.91 bit/s/Hz/core in spectral efficiency (SE). When sharing the parity-bit over 7 cores, the loss in SE becomes only 0.13 bit/s/Hz/core while the increase in transmission reach over PM-16QAM is 44 %.

© 2015 Optical Society of America

OCIS codes: (060.2330) Fiber optics communications; (060.4080) Modulation; (060.1660) Coherent communications.

References and links

1. B. Zhu, T. F. Taunay, M. Fishteyn, X. Liu, S. Chandrasekhar, M. F. Yan, J. M. Fini, E. M. Monberg, and F. V. Dimarcello, "112-Tb/s space-division multiplexed DWDM transmission with 14-b/s/Hz aggregate spectral efficiency over a 76.8-km seven-core fiber," *Opt. Express* **19**, 16665–16671 (2011).
2. J. Sakaguchi, B. J. Puttnam, W. Klaus, Y. Awaji, N. Wada, A. Kanno, T. Kawanishi, K. Imamura, H. Inaba, K. Mukasa, R. Sugizaki, T. Kobayashi, and M. Watanabe, "305 Tb/s space division multiplexed transmission using homogeneous 19-core fiber," *J. Lightwave Technology*, **31**, 554–562 (2013).
3. R. Ryf, S. Randel, A. H. Gnauck, C. Bolle, R. Essiambre, P. Winzer, D. W. Peckham, A. McCurdy, and R. Lingle, "Space-division multiplexing over 10 km of three-mode fiber using coherent 6×6 MIMO processing," in *Optical Fiber Communication Conference (OFC)* (2011), paper PDPB10.
4. E. Ip, N. Bai, Y. Huang, E. Mateo, F. Yaman, S. Bickham, H. Tam, C. Lu, M. Li, S. Ten, A. P. T. Lau, V. Tse, G. Peng, C. Montero, X. Prieto, and G. Li, "88×3×112-Gb/s WDM transmission over 50-km of three-Mode fiber

- with inline multimode fiber amplifier,” in *European Conference on Optical Communications (ECOC)* (2011), paper Th.13.C.2.
5. S. Jain, V. J. F. Ranaño, T. C. May-Smith, P. Petropoulos, J. K. Sahu, and D. J. Richardson, “Multi-element fiber technology for space-division multiplexing applications,” *Opt. Express* **22**, 3787–3796 (2014).
 6. K. Imamura, K. Mukasa, Y. Mimura, and T. Yagi, “Multi-core holey fibers for the long-distance (>100 km) ultra large capacity transmission,” in *Optical Fiber Communication Conference (OFC)*(2009), paper OTuC3.
 7. D. Qian, E. Ip, M. Huang, M. Li, A. Dogariu, S. Zhang, Y. Shao, Y. Huang, Y. Zhang, X. Cheng, Y. Tian, P. Ji, A. Collier, Y. Geng, J. Linares, C. Montero, V. Moreno, X. Prieto, and T. Wang, “1.05Pb/s transmission with 109b/s/Hz spectral efficiency using hybrid single- and few-mode cores,” in *Frontiers in Optics* (2012), paper FW6C.3.
 8. N. Amaya, S. Yan, M. Channegowda, B. R. Rofoee, Y. Shu, M. Rashidi, Y. Ou, E. Hugues-Salas, G. Zervas, R. Nejabati, D. Simeonidou, B. J. Puttnam, W. Klaus, J. Sakaguchi, T. Miyazawa, Y. Awaji, H. Harai, and N. Wada, “Software defined networking (SDN) over space division multiplexing (SDM) optical networks: features, benefits and experimental demonstration,” *Opt. Express* **4**, 715–723 (2012).
 9. D. Hillerkuss, R. Schmogrow, M. Meyer, S. Wolf, M. Jordan, P. Kleinow, N. Lindenmann, P. C. Schindler, A. Melikyan, X. Yang, S. Ben-Ezra, B. Nebendahl, M. Dreschmann, J. Meyer, F. Parmigiani, P. Petropoulos, B. Resan, A. Oehler, K. Weingarten, L. Altenhain, T. Ellermeyer, M. Moeller, M. Huebner, J. Becker, C. Koos, W. Freude, and J. Leuthold, “Single-laser 32.5 Tbit/s Nyquist WDM transmission,” *J. Optical Communications and Networking*, **24**, 1957–1960 (2012).
 10. R. Cigliutti, A. Nespola, D. Zeolla, G. Bosco, A. Carena, V. Curri, F. Forghieri, Y. Yamamoto, T. Sasaki, P. Poggiolini, “Ultra-long-haul transmission of 16x112 Gb/s spectrally-engineered DAC-generated Nyquist-WDM PM-16QAM channels with 1.05x(Symbol-Rate) frequency spacing,” in *Optical Fiber Communication Conference (OFC)* (2012), paper OTh3A.3.
 11. R. Ryf, R. Essiambre, S. Randel, A. H. Gnauck, P. J. Winzer, T. Hayashi, T. Taru and T. Sasaki, “MIMO-based crosstalk suppression in spatially multiplexed 3×56 -Gb/s PDM-QPSK signals for strongly coupled three-core fiber,” *Photonics Technology Letters*, **23**, 1469–1471 (2011).
 12. P. J. Winzer, “Spatial multiplexing: the next frontier in network capacity scaling,” in *European Conference on Optical Communications (ECOC)* (2013), paper We.1.D.1.
 13. M. D. Feuer, L. E. Nelson, X. Zhou, S. L. Woodward, R. Isaac, Z. Benyuan, T. F. Taunay, M. Fishteyn, J. M. Fini, and M. F. Yan, “Joint digital signal processing receivers for spatial superchannels,” *Photonics Technology Letters*, **24**, 1957–1960 (2012).
 14. E. Le Taillandier de Gabory, M. Arikawa, Y. Hashimoto, T. Ito, and K. Fukuchi, “A shared carrier reception and processing scheme for compensating frequency offset and phase noise of space-division multiplexed signals over multicore fibers,” in *Optical Fiber Communication Conference (OFC)* (2013), paper OM2C.2.
 15. M. Sjödin, P. Johannisson, H. Wymeersch, P. A. Andrekson, and M. Karlsson, “Comparison of polarization-switched QPSK and polarization-multiplexed QPSK at 30 Gbit/s,” *Opt. Express* **19**, 7839–7846 (2011).
 16. T. A. Eriksson, M. Sjödin, P. Johannisson, P. A. Andrekson, and M. Karlsson, “Comparison of 128-SP-QAM and PM-16QAM in long-haul WDM transmission,” *Opt. Express* **21**, 19269–19279 (2013).
 17. R. van Uden, C. Okonkwo, H. Chen, H. de Waardt, and A. Koonen, “6x28GBaud 128-SP-QAM transmission over 41.7 km few-mode fiber with a 6x6 MIMO FDE,” in *Optical Fiber Communication Conference (OFC)* (2014), paper W4J.4.
 18. T. A. Eriksson, P. Johannisson, M. Sjödin, E. Agrell, P. A. Andrekson and M. Karlsson, “Frequency and polarization switched QPSK,” in *European Conference on Optical Communications (ECOC)* (2013), paper Th.2.D.4.
 19. T. Koike-Akino, D. S. Millar, K. Kojima, and K. Parsons, “Eight-dimensional modulation for coherent optical communications,” in *European Conference on Optical Communications (ECOC)* (2013), paper Tu.3.C.3.
 20. T. A. Eriksson, P. Johannisson, E. Agrell, P. A. Andekson, and M. Karlsson, “Biorthogonal modulation in 8 dimensions experimentally implemented as 2PPM-PS-QPSK,” in *Optical Fiber Communication Conference (OFC)* (2014), paper W1A.5.
 21. A. D. Shiner, M. Reimer, A. Borowiec, S. Oveis Gharan, J. Gaudette, P. Mehta, D. Charlton, K. Roberts, and M. O’Sullivan, “Demonstration of an 8-dimensional modulation format with reduced inter-channel nonlinearities in a polarization multiplexed coherent system,” *Opt. Express* **22**, 20366–20374 (2014).
 22. D. S. Millar, T. Koike-Akino, S. Ö. Arık, K. Kojima, K. Parsons, T. Yoshida, and T. Sugihara, “High-dimensional modulation for coherent optical communications systems,” *Opt. Express* **22**, 8798–8812 (2014).
 23. T. A. Eriksson, P. Johannisson, B. J. Puttnam, E. Agrell, P. A. Andrekson, and M. Karlsson, “K-over-L multidimensional position modulation,” *J. Lightwave Technology*, **32**, 2254–2262 (2014).
 24. ITU-T, “Interfaces for the optical transport network,” ITU-T G.975 (2000).
 25. ITU-T, “Forward error correction for high bit-rate DWDM submarine systems,” ITU-T G.975.1 (2004).
 26. R.G. Gallager, “Low-density parity-check codes,” *IRE Transactions on Information Theory*, **8**, 21–28 (1962).
 27. D. Chang, F. Yu, Z. Xiao, Y. Li, N. Stojanovic, C. Xie, X. Shi, X. Xu, and Q. Xiong “FPGA verification of a single QC-LDPC code for 100 Gb/s optical systems without error floor down to BER of 10^{-15} ,” in *Optical Fiber Communication Conference (OFC)* (2011), paper OTuN2.
 28. H. Zhang, J.-X. Cai, H. G. Batshon, C. R. Davidson, Y. Sun, M. Mazurczyk, D. G. Foursa, A. Pilipetskii, G. Mohs,

- and Neal S. Bergano, "16QAM transmission with 5.2 bits/s/Hz spectral efficiency over transoceanic distance," *Opt. Express* **20**, 11688–11693 (2012).
29. J. Renaudier, P. Serena, A. Bononi, M. Salsi, O. Bertran-Pardo, H. Mardoyan, P. Tran, E. Dutisseuil, G. Charlet, and S. Bigo, "Generation and detection of 28 Gbaud polarization switched-QPSK in WDM long-haul transmission systems," *J. Lightwave Technology*, **30**, 1312–1318 (2012).
 30. D. S. Millar, T. Koike-Akino, K. Kojima, and K. Parsons, "A 24-Dimensional Modulation Format Achieving 6 dB Asymptotic Power Efficiency," in *Signal Processing in Photonic Communications (SPPCom)* (2013), paper SPM3D.6.
 31. B. J. Puttnam, J.-M. Delgado Mendinueta, R. S. Luís, T.A. Eriksson, Y. Awaji, N. Wada, and E. Agrell, "Single Parity Check Multi-Core Modulation for Power Efficient Spatial Super-channels," in *European Conference on Optical Communications (ECOC)* (2014), paper Mo.3.3.5.
 32. B. J. Puttnam, T. A. Eriksson, J.-M. Delgado Mendinueta, R. S. Luís, Y. Awaji, N. Wada, M. Karlsson, and E. Agrell, "Modulation Formats for Multi-Core Fiber Transmission," *Opt. Express* **22**, 32457–32469 (2014).
 33. M. Sjödin, P. Johannisson, J. Li, E. Agrell, P. A. Andrekson, and M. Karlsson, "Comparison of 128-SP-QAM with PM-16-QAM," *Opt. Express* **20**, 8356–8366 (2012).
 34. E. Agrell, and M. Karlsson, "Power-Efficient Modulation Formats in Coherent Transmission Systems," *J. Lightwave Technology*, **27**, 5115–5126 (2009).
 35. T. Pfau, S. Hoffmann, and R. Noé, "Hardware-Efficient Coherent Digital Receiver Concept With Feedforward Carrier Recovery for M -QAM Constellations," *J. Lightwave Technology*, **27**, 989–999 (2009).
 36. R. Elschner, F. Frey, C. Meuer, J. K. Fischer, S. Alreesh, C. Schmidt-Langhorst, L. Molle, T. Tanimura, and C. Schubert, "Experimental Demonstration of a Format-flexible Single-carrier Coherent Receiver Using Data-aided Digital Signal Processing," *Opt. Express* **20**, 28786–28791 (2012).
-

1. Introduction

Coherent detection together with digital signal processing (DSP) has enabled the use of spectrally efficient multilevel modulation formats in optical communication systems. For several reasons, quadrature phase shift keying (QPSK) is the most studied modulation format in coherent fiber optical communication systems. QPSK allows relatively low complexity transmitter, receiver and DSP design whilst also enabling transmission over transoceanic distances. For more spectrally efficient systems, 16-ary quadrature amplitude modulation (16QAM) is often considered as it offers a doubled spectral efficiency (SE) compared to QPSK and can be implemented with reasonable complexity.

Regardless of modulation format, the optical fiber and the amplifier technologies such as the Erbium-doped fiber amplifier (EDFA), Raman amplifiers, semiconductor amplifiers or amplification techniques based on nonlinear effects have a limited bandwidth, which determines the absolute maximum achievable data throughput. To increase the throughput of a single fiber link, space-division multiplexing (SDM) technologies such as multicore fibers (MCFs) and multimode fibers have recently received a tremendous research attention. Transmission over multicore fibers with, for instance, 7 cores [1] or 19 cores [2] as well as over multimode fibers [3, 4] have been demonstrated. Other promising SDM technologies exist, such as multi-element fibers [5], multicore holey fibers [6] and multicore fibers with few-mode cores [7].

In standard single mode fiber (SMF) transmission systems, data is packaged and routed on one wavelength division multiplexed (WDM) channel or as a superchannel consisting of a group of WDM channels [9, 10]. In SDM systems, the use of spatial superchannels has been proposed where data is routed in groups of the same wavelength over a number of cores or modes [8]. In strongly coupled systems with high levels of crosstalk, the use of spatial superchannels will be unavoidable since multiple-input multiple-output (MIMO) processing is required [11, 12]. The use of spatial superchannels also opens up for other possibilities such as joint DSP for phase recovery [13, 14].

The spatial superchannel also opens up the use of multidimensional modulation formats since the joint information of all spatial channels has to be accessible for the MIMO-processing. The use of four dimensional (4D) modulation formats such as polarization-switched QPSK (PS-QPSK) [15] and 128-ary set-partitioned QAM (128-SP-QAM) [16] has been shown to achieve

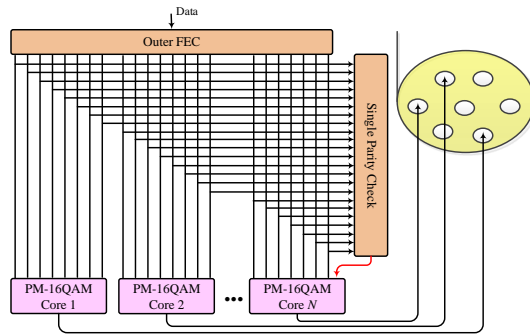


Fig. 1: Illustration of the principle of single parity check coded spatial superchannels for multicore fibers.

increased transmission distance over QPSK and PM-16QAM, respectively, at the cost of reduced SE. 128-SP-QAM has been investigated for SDM systems employing multimode fibers [17]. The optical field has four dimensions, given by polarization and quadratures, and for higher dimensional modulation formats, some method of increasing the dimensionality of the signal space has to be used. Eight dimensional (8D) modulation formats can be achieved utilizing two wavelength channels [18] or two consecutive time-slots [19, 20, 21]. Further, higher dimensional modulation formats has been studied based on sphere cutting or block coding [22] or multidimensional position modulation [23]. These modulation formats could as well utilize the dimensions spanned by the spatial superchannel.

Forward error correction (FEC) codes has been a key-technology for coherent fiber optical communication systems enabling a pre-FEC bit-error-rates (BERs) in the region of 10^{-3} . Traditionally, FEC codes based on Reed-Solomon (RS) [24] or Bose-Chaudhuri-Hocquengham (BCH) [25] codes have been the dominating technology in the fiber optical community. However, recently a lot of research has been devoted to applying more advanced soft-decision FEC coding schemes typically based low-density parity check (LDPC) codes [26, 27, 28]. When modulation is considered over a high dimensional signal space the definition of modulation formats and forward error correcting (FEC) codes becomes blurred. Many high-dimensional modulation formats can be constructed as a low-dimensional modulation format in combination with an FEC code, which determines which sequences of low-dimensional symbols are allowed. For instance, PS-QPSK is a single parity-check (SPC) code on PM-QPSK [29] and 128-SP-QAM a SPC code on PM-16QAM [16]. Further, the extended Golay code, which is a well-known rate-1/2 FEC code, was applied to PM-QPSK in six consecutive time slots, thus yielding a 24-dimensional modulation format with 4096 points [30].

In this paper we experimentally investigate SPC codes over spatial superchannels for multicore fiber utilizing PM-16QAM. PM-16QAM offers a high SE but the achievable transmission distances are much more limited compared to PM-QPSK. This makes the use of the low-complexity SPC code for increased sensitivity, which translates into increased transmission reach at a cost of a slight reduction in SE, an interesting alternative for PM-16QAM. We have previously investigated this concept for QPSK signals and shown that the required OSNR could be improved by up to 1.8 dB with minimum reduction of the SE [31, 32]. SPC coded PM-16QAM over one core has a reduced SE of 7/8 compared to PM-16QAM, and increasing the number of cores that the SPC is applied over, increases the SE since the parity-bit can be shared among more parallel channels.

In this contribution, we take this concept further by experimentally investigate the SPC coded

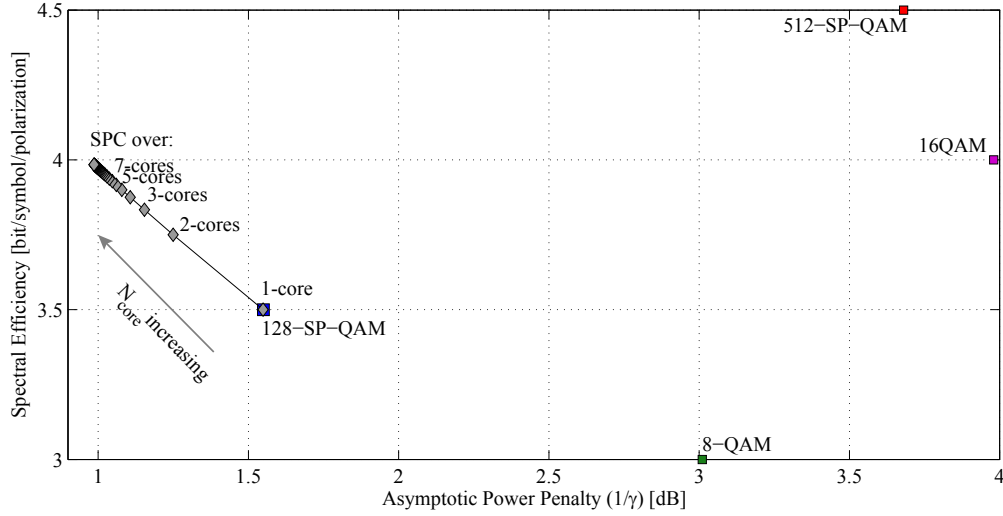


Fig. 2: Spectral Efficiency as a function of the asymptotic power penalty ($1/\gamma$) for some known formats as well as for the SPC-16QAM formats (grey diamonds) with the SPC ranging from being applied over 1 (equivalent to 128-SP-QAM) to 100 cores.

formats for spatial superchannels consisting of 20 GBaud PM-16QAM signals on a WDM grid of 22 GHz over a 7-core fiber. In back-to-back experiments we show a 1.1 dB increased sensitivity at $\text{BER} = 10^{-3}$ using the SPC over 7 cores. In recirculating loop experiments we show that with the 22 GHz WDM spacing, using SPC over 1 core can achieve more than double transmission distance compared to PM-16QAM at the cost of 0.91 bit/s/Hz/core. Further, when sharing the parity-bit over the all 7 cores, the loss in SE is only 0.13 bit/s/Hz/core while the increase in transmission reach over PM-16QAM is 44 %.

2. Single parity check encoding and decoding

The SPC code is an extremely low complexity FEC code. The encoding is done by adding one parity bit to n_{ib} number of information bits, b_1, b_2, \dots, b_n . The parity bit is encoded as an modulo-2 addition on the n_{ib} information bits such that

$$b_{\text{SPC}} = b_1 \oplus b_2 \oplus \dots \oplus b_{n-1} \oplus b_{n_{ib}} \quad (1)$$

where the symbol \oplus denotes the modulo-2 addition, which is an XOR-operation. In this paper we use PM-16QAM in each core of the spatial superchannel which gives a total number of information bits

$$n_{ib} = 8N_{\text{core}} - 1 \quad (2)$$

where N_{core} is the number of cores over which the SPC is applied, the 8 comes from the fact that PM-16QAM carries 8 bits per symbol and the -1 results from the SPC-bit. This concept is illustrated in Fig. 1, where the SPC is performed over the full superchannel. The SPC can be performed on a lower number of cores, dividing the MCF into groups of cores where the SPC is applied. If the SPC is applied on a core-to-core basis, this is equivalent to transmitting 128-SP-QAM in each core [16]. To decode the SPC, a soft-decision FEC decoder that minimizes the Euclidean distance between the received vector and the decoded codewords, is used in the receiver. This decoder is equivalent to the maximum-likelihood decoder for the AWGN channel. An efficient decoder implementation was discussed in [33]

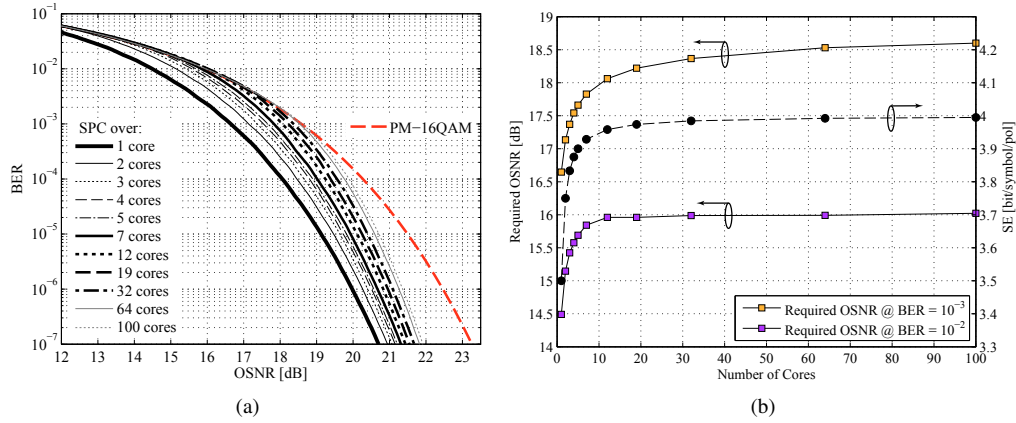


Fig. 3: (a) Simulations with AWGN as the only impairment for PM-16QAM (red dashed line) and SPC-16QAM where the SPC is performed over 1, 2, 3, 4, 5, 7, 12, 19, 32, 64, and 100 cores for a symbol rate of 20 Gbaud (b) Required OSNR for BER = 10^{-3} (orange squares) and BER = 10^{-2} (purple squares) as a function of the number of cores over which the SPC is performed. Also shown, SE as a function of the number of cores (black circles).

To compare the SPC formats to other modulation formats, we use the SE and the asymptotic power efficiency (APE) [34]. The APE, often referred to as γ , gives the sensitivity gain over QPSK at asymptotically low BERs and is defined as

$$\gamma = \frac{d_{\min}^2 \log_2 M}{4E_s}, \quad (3)$$

where d_{\min} is the minimum Euclidean distance, M is the number of constellation points, E_s is the average symbol energy and the factor 1/4 normalizes the APE to QPSK. The SE is defined as

$$SE = \frac{\log_2 M}{N/2} = \frac{\log_2 M}{2N_{\text{core}}}, \quad (4)$$

where N is the number of dimensions and $N = 4N_{\text{core}}$ for coherent 4D-modulation. As a reference, we note that QPSK has an APE of 0 dB and an SE of 2 bit/symbol/polarization. For the SPC-16QAM formats $M = 2^{8N_{\text{core}}-1}$ and $E_s = \epsilon_s N_{\text{core}}$, where ϵ_s is the average symbol energy per core. Using this, and Eq. (3) and Eq. (4), it can be shown that the APE for the SPC-16QAM formats can be expressed as

$$\gamma_{\text{SPC-16QAM}} = \frac{2d_{\min}^2}{\epsilon_s} - \frac{d_{\min}^2}{4\epsilon_s N_{\text{core}}} = 2\gamma_{16\text{QAM}} \left(1 - \frac{1}{8N_{\text{core}}}\right), \quad (5)$$

and the SE as

$$SE_{\text{SPC-16QAM}} = 4 - \frac{1}{2N_{\text{core}}} = SE_{16\text{QAM}} \left(1 - \frac{1}{8N_{\text{core}}}\right). \quad (6)$$

The SE and asymptotic power penalty ($1/\gamma$) for 16QAM, rectangular 8-QAM, 128-SP-QAM and 512-SP-QAM, as well as for the SPC-16QAM formats with the number of cores, N_{core} , ranging from 1 to 32, are plotted in Fig. 2. As shown in Fig. 2, it is possible to simultaneously increase both the SE and the APE by increasing the number of cores that the SPC is applied over. Using a 7-core fiber and applying the SPC over all cores, the APE is -1.047 dB and the

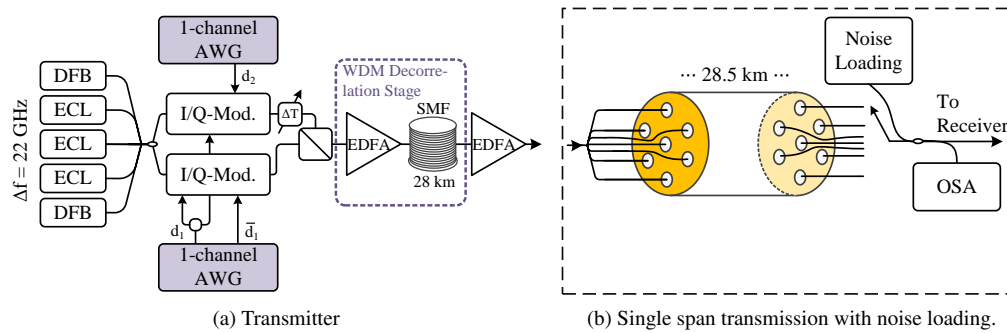


Fig. 4: (a) Transmitter used for both PM-16QAM and all SPC-16QAM formats. (b) Setup for single span transmission with noise loading.

SE is 3.929 bit/symbol/polarization and for a 19-core fiber the APE is -0.998 dB and the SE is 3.974 bit/symbol/polarization. When N_{core} approaches infinity, the APE goes to -0.969 dB, which is a 3 dB improvement over 16QAM, and the SE goes to 4 bit/symbol/polarization which is the same as for 16QAM.

Since modern coherent optical communication systems typically utilizes FEC which operates at pre-FEC BER targets in the region around 10^{-3} to 10^{-2} , investigating only the APE is not enough to find suitable modulation formats. To find the performance of the SPC in the low BER region, we perform simulations with additive white Gaussian noise (AWGN) as the only impairment. The results for SPC over 1, 2, 3, 4, 5, 7, 12, 19, 32, 64, and 100 cores for a symbol rate of 20 Gbaud are shown Fig. 3(a). For comparison, the result for PM-16QAM is also shown. In the same fashion as the APE in Fig. 2, the sensitivity gain is saturating with increasing core over which the SPC is performed. This is more clear in Fig. 3(b), where the required OSNR for a BER of 10^{-3} (orange squares) and 10^{-2} (purple squares) are shown as a function of the number of cores over which the SPC is performed. It should be noted that these simulations (and the experiments performed in this paper) are performed at the same symbol rate of 20 Gbaud as opposed to the definition APE used in Fig. 2 where the same bitrate is assumed. We use the same symbol rate since in a realistic scenario, the complexity of a spatial superchannel system would be much higher if the bitrate and/or the channel spacing should be flexible with the number of channels the SPC is applied over. As seen in Fig. 3(b), there is a large sensitivity gain for performing the SPC over a low number of cores and the sensitivity gain is diminishing and saturating when the number of cores are increased. However, as seen in the plot of the SE as a function of the number of cores (black circles), with increasing number of cores the SE is also increased since the parity bit is shared over more cores. Also, we note that the sensitivity gain is reduced if operating at a pre-FEC BER of 10^{-2} opposed to BER of 10^{-3} and that at the lower BER, the saturation in sensitivity gain occurs faster.

3. Experimental setup

The experimental setup is shown in Fig. 4 and Fig. 5. The transmitter, shown in Fig. 4(a) consisted of two I/Q-modulators for polarization diverse modulation. As a light source a 530 kHz linewidth tunable external cavity laser (ECL) was used for the center channel. Two more ECLs, identical to the center channel laser, in combination with two distributed feedback lasers (DFBs) with ~ 1 MHz linewidth, i.e. in total 5 channels, were used to emulate a WDM-transmission link with a channel spacing of 22 GHz.

The I/Q-modulators were driven by four-level signals generated from two arbitrary waveform

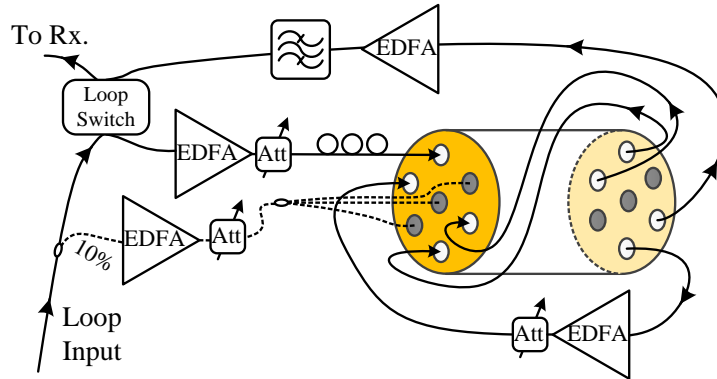


Fig. 5: Experimental setup for the multicore fiber recirculating loop utilizing two cores for transmission and the other 5 cores are loaded with dummy channels (gray).

generators (AWGs) with 50 GS/s sample rate and 14 GHz electrical bandwidth. The pulse shape used was root-raised cosine with a roll-off factor of 0.1. Since only two independently programmable channels were available, three of the driving signals had to be derived from the differential outputs of one AWG and the last driving signal, which was used to generate the signal containing the SPC bit sequence, was generated by a separate AWG as indicated in Fig. 4(a). All four electrical signals were amplified using linear driving amplifiers with 30 GHz bandwidth. Pre-equalization of the electrical signals was performed using FIR filters computed to compensate the limited response of the AWGs and other transmitter components. However, only two individual AWG channels were available, and different cable lengths, splitters and RF delay lines caused the response of the four paths to be slightly different. Hence, a small difference in the performance of the four signals was observed.

The signals from the two I/Q-modulators were combined with orthogonal polarizations using a polarization beam combiner which was followed by an amplification stage. A tunable optical delay was used in one arm to align the transmitted bit slots. To decorrelate the WDM channels, the transmitter stage was followed by an SMF with a length of 36 km. The launch power into the SMF was kept below -5 dBm to reduce the impact of introducing non-linear impairments in this stage. However, it should be noted that this is suboptimal since the decorrelation between two neighboring WDM channels only corresponds to roughly 2 symbol slots. However, since further decorrelation occurs from the use of free-running transmitter lasers and a non-dispersion managed link in addition to the SMF, this was not considered problematic.

The setup for single-span measurement with noise loading is shown in Fig. 4(b). The signal corresponding to the signal to be transmitted through a specific core was loaded in the AWGs. This signal was then split into seven branches that were decorrelated by fibers of different lengths before being launched into each core of the 28.5 km 7-core fiber such that six channels acted as dummy channels for realistic crosstalk levels. An optical switch was used after the MCF to pick out the signal from one core. This signal was then sent to a noise loading stage, consisting of concatenated EDFAs and optical bandpass filters, before being sent to the coherent receiver.

The setup for recirculating loop experiments is shown in Fig. 5. The loop consisted of two spans, constructed from the same 28.5 km 7-core fiber. Each span was constructed from two opposite cores in the MCF, with all cores using the same propagation direction. Hence, the span length before amplification was 57 km and the total loop length was 114 km. The remaining 3 cores were loaded with dummy signals tapped from the signal before it entered the loop. The

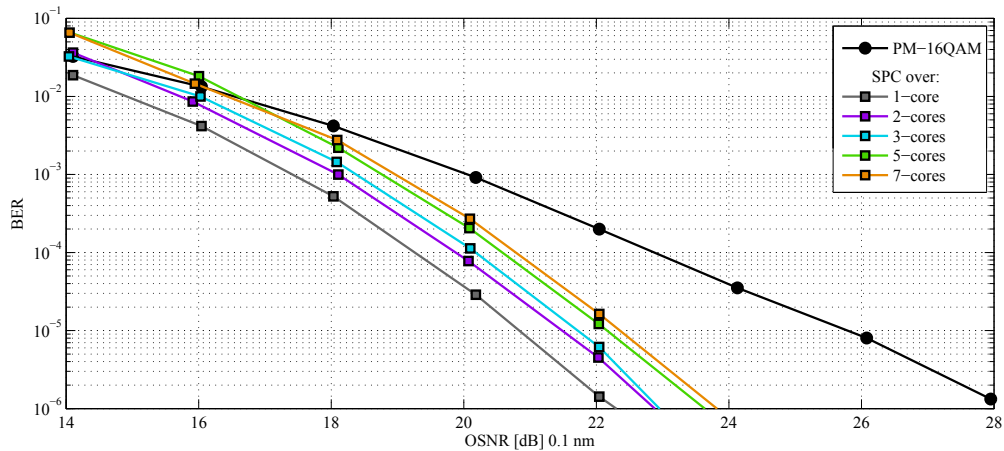


Fig. 6: Measured BER as a function of OSNR through a single span 27.5 km MCF for 20 Gbaud PM-16QAM and 20 Gbaud SPC-16QAM over 1, 2, 3, 5, and 7 cores.

launch power of the dummy signals were adjusted to match that of the signal in the loop. Each span was preceded by an EDFA which was followed by a variable attenuator and a 20 dB tap to control the launch power into each span. A tunable optical bandpass filter was used in the loop to suppress out of band amplified spontaneous emission (ASE) as well as a third EDFA which compensates for the loss of the loop switching components and the filter.

The receiver consisted of a tunable optical bandpass filter followed by an EDFA before a polarization diverse coherent receiver with an electrical bandwidth of 33 GHz and a sample rate of 80 GS/s. The linewidth of the local oscillator (LO) laser was 100 kHz. Due to the lack of seven synchronized receivers and transmitters, the signal in each core had to be modulated and detected in turn. The received signals were stored and processed off-line as described in the following section.

3.1. Digital signal processing

The DSP starts with optical front-end corrections and resampling to 2 samples/symbol followed by electronic dispersion compensation. The adaptive equalizer and polarization demultiplexing is based on four butterfly-configured finite impulse-response filters with 17 taps. The filters are first updated using the constant modulus algorithm for pre-convergence and is then switched to decision-directed least-mean square (DD-LMS) for final adaptation. Frequency offset compensation using the fast-Fourier transform and carrier phase estimation based on blind phase search with 32 test angles is performed within the DD-LMS loop [35]. For all formats, 16QAM constellations are used as reference, i.e. all formats uses exactly the same DSP until the demodulation stage. For the SPC formats, the bits are first detected using the same hard-decision as for 16QAM to find the symbols where the parity is not matching. The symbols with erroneous parity are detected using the minimum Euclidean distance to the SPC-16QAM symbols.

4. Experimental results

The BER as a function of OSNR for a single WDM channel with 20 Gbaud PM-16QAM as well as 20 Gbaud SPC-16QAM over 1, 2, 3, 5, and 7 cores, transmitted through a single span of MCF with noise loading (Fig. 4(b)) is shown in Fig. 6. Please note that in this and following figures, some batches have been removed from the plots where the DSP did not converge, suffered

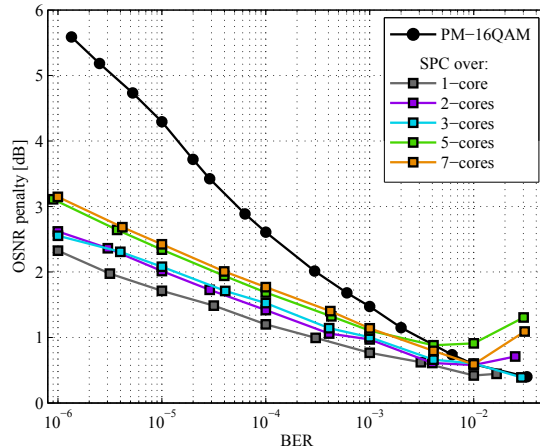


Fig. 7: Implementation penalty at different pre-FEC BER targets.

from a phase slip in the phase tracking, or the synchronization of the different batches were erroneous. We note that although not performed here, these problems could be solved using data-aided training sequences similar to [36]. Since we use the same transmitter and DSP for all formats, we do not expect a difference in phase-slip probability for the different formats. The implementation penalty, defined as the OSNR penalty compared to simulations with AWGN as the only impairment is plotted in Fig. 7. At $\text{BER} = 10^{-3}$, the implementation penalty for PM-16QAM was 1.5 dB and for SPC-16QAM over one core it was 0.8 dB. For SPC-16QAM the implementation penalty ranged from 1.0-1.1 dB for 2, 3, 5 and 7 cores.

We note that for low OSNR where the BER is higher than 10^{-2} , the SPC-16QAM formats seem to suffer extra penalty, especially for 5 and 7 cores which see an increase in implementation penalty at the high BERs. This is also seen in Fig. 6, where SPC-16QAM over 5 and 7 cores has an inferior sensitivity compared to PM-16QAM at OSNR lower than 16.7 dB and 16.1 dB, respectively. It is clear that SPC is best used in combination with an FEC code operating around 10^{-3} , which is typical for hard-decision FEC codes [24, 25]. Furthermore, for systems without strong FEC, the SPC-16QAM formats are good candidates showing for instance 3.4 dB gain in sensitivity at $\text{BER} = 10^{-5}$ using 7 cores compared to PM-16QAM. This gain is expected to increase even further at lower BERs. At $\text{BER} = 10^{-3}$, the measured sensitivity gain over PM-16QAM is 2.7 dB for 1-core SPC-16QAM, 2.0 dB 2-core SPC-16QAM, 1.7 dB for 3-core SPC-16QAM, 1.3 dB for 5-core SPC-16QAM, and 1.1 dB for 7-core SPC-16QAM.

Fig. 8 shows the transmission results with BER plotted as a function of transmission distance in the recirculating loop for different launch powers. The results are shown for the following formats; 20 Gbaud PM-16QAM in single channel transmission (a) and in a 22 GHz WDM grid (b). SPC-16QAM where the SPC is performed over 1 core for single channel transmission (c), and in a 22 GHz grid (d). SPC-16QAM where the SPC is performed over 3 cores for single channel (e), and with 22 GHz WDM spacing (f). Lastly, SPC-16QAM over 7 cores is shown for single channel (g) and in a 22 GHz grid (h). The optimal launch power into each core was -3 dBm for all formats in single channel transmission and -4 dBm for all formats in WDM transmission. We also note that the penalty from suboptimal launch powers is similar for all cases.

4.1. Single channel transmission

At $\text{BER} = 10^{-3}$, the achievable transmission distance in single channel transmission was 700 km for PM-16QAM. It should be noted that the transmission distance is limited by a combination of crosstalk in the MCF as well as losses in the loop switch which becomes more significant due to the short loop length. For SPC-16QAM over 1 core, the transmission distance is increased by 56 % to 1090 km. We note that SPC over 1 core is the same modulation format as 128-SP-QAM and that the increase in transmission distance over PM-16QAM agrees well with what was seen in single-core transmission [16]. Using SPC over 3 cores, the achievable distance in single channel transmission is 910 km which is an increase of 30 % over PM-16QAM and using SPC over 7 cores yields a transmission distance of 845 km which corresponds to 21 % increase over PM-16QAM.

4.2. WDM transmission

From Fig. 8(b), it is seen that the achievable transmission distance for PM-16QAM for the optimal launch power at $\text{BER} = 10^{-3}$ was 390 km with a 22 GHz WDM grid. Using SPC over 1 core, the achievable transmission distance was 870 km with WDM (Fig 8(d)). Interestingly, the WDM penalty compared to the single channel case is larger for PM-16QAM than with SPC over 1 core, as the transmission distance is reduced by 44 % for PM-16QAM compared to a reduction of 20 % for 1-core SPC-16QAM. Again this agrees with the results in [16], where a larger penalty occurs for moving from single channel transmission to WDM transmission for PM-16QAM compared to 128-SP-QAM.

For a 22 GHz WDM spacing, the transmission distance is increased by 123 % using SPC over 1 core compared to PM-16QAM at the same WDM spacing. With SPC over 3 cores (Fig. 8(e)), the achievable transmission distance at $\text{BER} = 10^{-3}$ was 710 km in WDM transmission. As expected, the transmission distance is reduced compared to 1-core SPC-16QAM. However, compared at the 22 GHz WDM spacing, the transmission distance is still increased by 82 % over PM-16QAM. Finally, using SPC over 7 cores (Fig. 8(h)) the achievable transmission distance in WDM transmission is 560 km which corresponds to an increase in transmission distance of 44 % over PM-16QAM at the same WDM spacing.

In Table 1, the achievable transmission distance at $\text{BER} = 10^{-3}$ and the pre-FEC SE for the 22 GHz WDM spacing cases is listed. As seen, the largest gain in transmission distance is using the SPC format over one core. However, this comes at the loss of 0.91 bit/s/Hz/core of SE. Using the SPC over 7 cores, this loss becomes only 0.13 bit/s/Hz/core but in this case the gain in transmission reach is reduced significantly. The 3-core SPC-16QAM is an intermediate case with 0.30 bit/s/Hz/core loss in SE compared to PM-16QAM and significant gain in transmission

Table 1: Experimental SE and Achievable Transmission Distance

Modulation Format	SE ^a	Transmission Distance ^b
PM-16QAM	7.27 bit/s/Hz/core	390 km
1-core SPC-16QAM	6.36 bit/s/Hz/core	870 km
3-cores SPC-16QAM	6.97 bit/s/Hz/core	735 km
7-cores SPC-16QAM	7.14 bit/s/Hz/core	560 km

^a Pre-FEC SE with 22 GHz WDM spacing.

^b at $\text{BER} = 10^{-3}$.

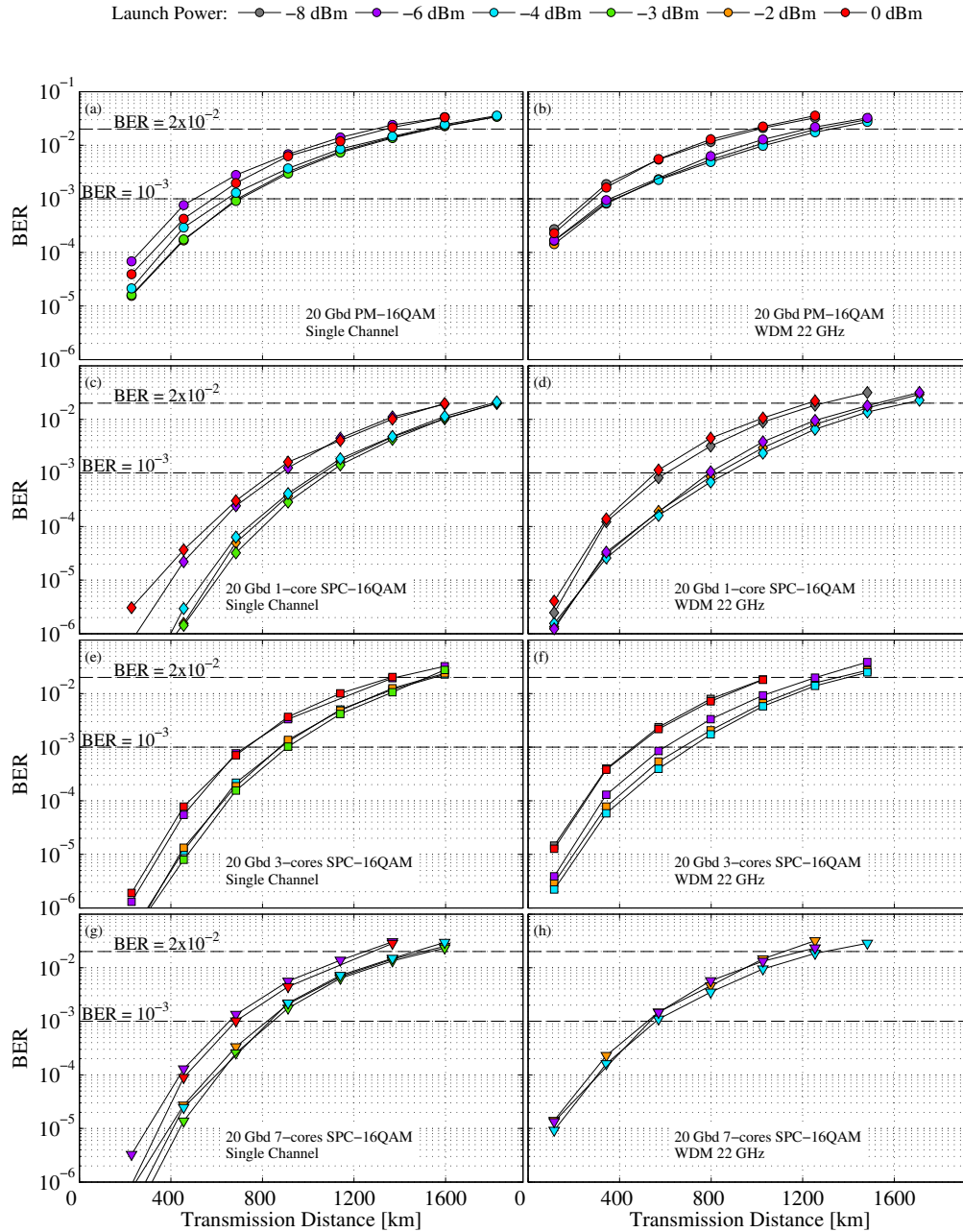


Fig. 8: Experimental transmission results showing BER as a function of transmission distance for different launch powers for: 20 Gbaud PM-16QAM for (a) single channel and (b) WDM transmission with 22 GHz spacing. SPC-16QAM over 1 core for (c) single channel and (d) WDM. SPC-16QAM over 3 cores for (e) single channel and (f) WDM. SPC-16QAM over 7 cores for (g) single channel and (h) WDM transmission.

reach. Hence, these results clearly demonstrates the trade-off between SE and increase in transmission distance over PM-16QAM for the SPC formats. This can also be expected comparing to the measurement of SPC in combination with PM-QPSK in [31, 32].

4.3. Performance at higher Pre-FEC BER targets

FEC codes operating at a pre-FEC BER in the region of 10^{-3} are often using hard-decision decoding [25, 24] and are of lower complexity compared to soft-decision codes such as LDPC codes which can typically operate at a pre-FEC BER around 10^{-2} [26, 27]. As stated in previous sections, the SPC formats are best used FEC codes operating at a pre-FEC BER of about 10^{-3} . However, it is still interesting to compare the formats at a high pre-FEC BER target since there might be situations where these formats could be used in combination with an advanced FEC code, say as a backup in degrading links where the FEC circuitry would be fixed. With that we note that for advanced FEC, it is highly likely that more gain in terms of transmission distance would be achieved from using all the overhead for a more powerful code. In this section, we choose to compare the formats at a pre-FEC BER target of $\text{BER} = 2 \times 10^{-2}$.

In this case, single channel PM-16QAM can be transmitted up to 1540 km and 1-core SPC-16QAM up to 1830 km. Further, 3-core SPC-16QAM can be transmitted 1550 km and 7-core SPC-16QAM up to 1540 km (Figs. 8(a), 8(c), 8(e), and 8(g)). As seen, 1-core SPC still achieves a longer transmission distance but the gain is much smaller compared to at $\text{BER} = 10^{-3}$. The achievable distance for 3-core SPC-16QAM and 7-core SPC-16QAM is roughly the same as PM-16QAM. Hence, at this pre-FEC BER target PM-16QAM is preferable over 3-core and 7-core SPC-16QAM since the SE is higher for PM-16QAM.

For WDM transmission with a 22 GHz grid spacing (Figs. 8(b), 8(d), 8(f), and 8(h)), the transmission distance for PM-16QAM is reduced to 1320 km compared to the single channel case. The corresponding number is 1655 km for 1-core SPC-16QAM, 1400 km for 3-core SPC and 1295 km for 7-core SPC-16QAM. Again, the transmission distance for 3-core SPC-16QAM is similar to that of PM-16QAM and 7-core SPC-16QAM even has a reduced transmission distance compared to PM-16QAM. However, this is no surprise since we know from the back-to-back results in Fig. 6 that the measured sensitivity for 7-core SPC-16QAM was worse compared to PM-16QAM at this BER.

At $\text{BER} = 2 \times 10^{-2}$ the WDM penalties compared to single channel transmission for all formats are not as distinctive compared to what we saw at $\text{BER} = 10^{-3}$. However, we note that PM-16QAM still sees a larger WDM penalty compared to all SPC formats except 7-core SPC which has roughly the same penalty as PM-16QAM.

5. Conclusions

We have experimentally investigated modulation formats based on SPC over spatial-superchannels consisting of 20 Gbaud PM-16QAM signals for long-haul multicore transmission systems. By sharing the parity-bit over several cores, the loss in SE can be reduced while there is still gain in terms of sensitivity.

We conclude that these formats are best used in systems where an FEC code operating around BER around 10^{-3} , or lower, is preferred, which is the case for many hard-decision FEC codes. The reason for this is that at this pre-FEC BER target, significant sensitivity gain over PM-16QAM can be achieved.

We investigated the SPC formats in MCF transmission and using 22 GHz WDM spacing we found that with SPC over 1 core, the transmission distance can be increased by 123 % compared to PM-16QAM at the cost of a 0.91 bit/s/Hz/core lower SE. Using SPC over 7 cores, the loss in SE is only 0.13 bit/s/Hz/core compared to PM-16QAM with 44 % increased transmission distance.

Acknowledgments

This work was partially funded by The Swedish Research Council (VR). Tobias A. Eriksson would like to acknowledge the financial support from Ångpanneföreningens Forskningsstiftelse as well as from the Sweden-Japan Foundation with support from Mitsubishi.